p ISSN 1907-0322
e ISSN 2527-6433

Effect of Filter on Image Reconstruction using Filtered Back Projection Algorithm for Industrial Gamma-Ray Tomography Technique

Pengaruh Filter pada Rekonstruksi Citra Menggunakan Algoritma Filtered Back Projection untuk Teknik Tomografi Sinar Gamma Industri

Bayu Azmi*, Wibisono, Darman, Sugiharto

Center for Isotopes and Radiation Application, National Nuclear Energy Agency (BATAN)
Jl. Lebak Bulus Raya No. 49, Jakarta 12440, Indonesia
* e-mail : bayuazmi@batan.go.id

ABSTRACT

Gamma-ray tomography experiment has been carried out to detect the cross-sectional spatial patterns of test objects. The resulting image quality depends on the data collection and image reconstruction process. The images were built using filtered back projection algorithm. The filter in the algorithm affects the resulting image. It is necessary to know the proper filter when reconstructing image using the algorithm. Data were collected by scanning the object using the parallel beam method. Scanning configuration was set up to every 5 mm and 32 projections (rotational scans). The scanning system consists of mechanical parts, computerized control module, a gamma-ray source (2.96 GBq of Cs-137), a NaI(Tl) scintillation detector, data acquisition and computer. In this paper, the data were reconstructed into images using back projection and also filtered back projection algorithm to study effect of the filters. The filters discussed are Ramp filter, Shepp-Logan filter, Hann filter, Hamming filter, and Cosine filter. The reconstructed images results with filter were much better than without filter. The images with no filter did not represent the object cross-sectional spatial patterns and looked blurred. There were only solid objects represented by bright white and air represented by dark colors. The images using filter could distinguish object based on its density. Ramp filtered images looked like it was filled with freckles. Shepp-Logan filter produced smoother images than Ramp filter. Hann, Hamming, and Cosine filtered images were smoother than the others. Hann and Hamming filters produced higher resolution images regarding to recognizing density value. Hann filtered images also has the smallest standard deviation. Overall, Hann filter is recommended to be used to reconstruct images from projections.

Keywords: Back projection algorithm, filter, gamma-ray tomography, image reconstruction, industry

ABSTRAK

Percobaan tomografi sinar gamma telah dilakukan untuk mendeteksi pola spasial penampang lintang dari beberapa obyek uji. Kualitas dari citra yang dihasilkan bergantung pada proses pengambilan data dan proses rekonstruksi citra. Citra dibangun menggunakan algoritma *filtered back projection.* Filter yang digunakan pada algoritma tersebut mempengaruhi citra yang dihasilkan. Penting untuk mengetahui filter yang tepat pada saat merokonstruksi citra menggunakan algoritma tersebut. Proses pengambilan data dilakukan dengan cara memindai obyek dengan metode *parallel beam*. Konfigurasi pemindaian diatur setiap 5 mm dan sebanyak 32 proyeksi (pemindaian rotasi). Sistem pemindaian terdiri dari bagian mekanik, modul pengendali terkomputerisasi, sebuah sumber gamma (Cs-137 dengan aktivitas 2,96 GBq), sebuah detektor sintilasi NaI(Tl), sistem akuisisi data, dan komputer. Pada paper ini, data hasil pemindaian direkonstruksi menjadi citra menggunakan algoritma *back projection* dan *filtered back projection* untuk mempelajari pengaruh filter terhadap citra. Filter-filter yang didiskusikan adalah *Ramp filter*, *Shepp-Logan filter*, *Hann filter, Hamming filter,* dan *Cosine filter*. Citra hasil rekonstruksi dengan menggunakan filter jauh lebih baik dibandingkan tanpa menggunakan filter. Citra tanpa menggunakan filter tidak menggambarkan pola spasial penampang lintang dari obyek dan terlihat blur. Hanya terdapat obyek padat yang berwarna putih terang dan udara yang berwarna gelap. Sedangkan hasil citra dengan menggunakan filter mampu membedakan densitas dari obyek. Citra *Ramp filter* terlihat dipenuhi bintik-bintik. *Shepp-Logan filter* menghasilkan citra yang lebih halus dibanding *Ramp filter.* Citra menggunakan *Hann, Hamming,* dan *Cosine filter* lebih halus dibanding lainnya. *Hann* dan *Hamming filter* menghasilkan citra beresolusi tinggi terkait kemampuan membedakan nilai densitas. Citra dengan *Hann filter* juga memiliki deviasi standar yang paling kecil. Secara keseluruhan, *Hann filter* direkomendasikan untuk merekonstruksi citra dari proyeksi.

Kata kunci: Algoritma *back projection*, filter, tomografi sinar gamma, rekonstruksi citra, industri

p ISSN 1907-0322
e ISSN 2527-6433

INTRODUCTION

The ability to check the internal structure of an object is necessary in industrial processes to diagnose malfunctions or in order to increase the production [1]. One technique that is being used to detect the internal structure of an object is tomography. Tomography is an advanced technique that has been continuously developed and being used for diagnostic purposes throughout last 40 years not only in medic but also in industry, biology and civil engineering applications [2]. Tomography started with the theoretical justification of the possibility of reconstructing the distribution of a certain parameter across a planar section of an object from its projections [3]. It produces two or three-dimensional cross-sectional images of an object. For industrial purpose, a transmitter which has a capability to penetrate high density material is required.

Gamma-ray has been widely used for diagnosing and measuring system for industrial application such as radioisotope tracer techniques, fluid density measurement, and column scanning [4], [5], [6]. The advantages of using gamma-ray are its high energy and it does not require a power generator to emit radiation like X-ray machine. High energy increases the probability of gamma photons to penetrate the material with high density that make it possible to be utilized for diagnostic in the industry.

The Cs-137 is commonly used for nuclear gauging application because its long half-life, does not scatter interference of photons of other energies and emits single clear photo peak [7]. It has a half-life of 30.23 years and decays β-particles only, producing Ba-137, which creates all the γ-ray emissions with energy peak of 662 keV [8]. Cs-137 energy is effective for penetrating metal materials and can distinguish the density quite well.

The parallel beam gamma-ray tomography method was used in this experiment. A collimated gamma source emits photons which then penetrate the object to be scanned by the detector on the other side. This method is also called transmission tomography. The tomography system scans the object in translation and rotation. The scanning process produces projections data of the object.

Gamma-ray transmission tomography attempts to image density distribution inside the object area by measuring the attenuation of gamma radiation [9]. When gamma-rays penetrate materials with variable thickness, the result should follow exponential attenuation based on the Lambert-Beer law [10]:

$$\frac{I}{I_0} = e^{-\mu x} \quad (1)$$

where I (CPS) is radiation intensity after penetrating materials, I_0 (CPS) is the intensity of incident radiation, μ is the linear attenuation coefficient, and x (m) is material thickness.

The projections data are being used to reconstruct image using filtered back projection algorithm. Back projection algorithm processes images one by one, cummulatively adding the densities of current image to the densities of all previous projection images, and gradually building up the 2D or 3D density distribution of the particle [11]. The main weakness of back projection algorithm is it produces a blurred image. Filtered back projection algorithm designed to resolve the limitation of back projection algorithm. It applies a convolution filter to remove blurring. This paper discusses the effect of filter on the filtered back projection algorithm. The filters discussed are Ramp filter, Shepp-Logan filter, Hann filter, Hamming filter and Cosine filter.

MATERIALS AND METHODS

Gamma tomography scanning system

The scanning system consisted of a Cs-137 gamma source, a NaI(Tl) scintillation detector, counter system, mechanical system, computerized control module, data acquisition, and a computer as shown in Figure 1 [1]. The gamma radiation source was encapsuled and placed in a lead collimator during the experiment. A collimated scintillation detector on the other side of the object counted the radiation emitted by the radiation source. Gamma source collimator aimed to direct gamma ray into narrow beam and for radiation safety purposes, whereas the detector collimator to block scaterred radiation detected by detector. The collimators slit diameter was 5 mm. The gamma tomography system uses a higher energy than the X-ray CT and is capable of measuring objects with larger dimensions [12].

p ISSN 1907-0322
e ISSN 2527-6433

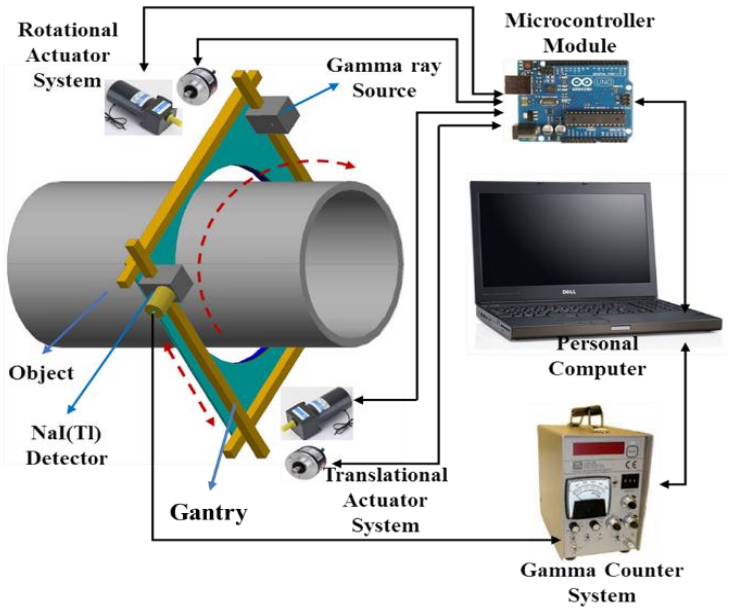

Figure 1. Gamma tomography scanning system

The system was designed to conduct translational and rotational scan automatically. The translational scan aimed to get the projection data profile of the object at a certain projection position by moving source and the detector on the gantry in parallel. Rotational scan was to rotate the gantry to the next projection and conduct translational again to get the next projection data.

Experiment

Data collection process was done by scanning the object in translation and rotation. Azmi et.al. [13] have scanned several objects using the parallel beam gamma tomography system. In this paper we used two objects as shown in Figure 2. Both objects are scanned with 32 projections in 180^0. That means the gantry will rotate 5.625^0 every rotational step.

Object #1 was geothermal power plant pipe with scale inside it. Pipe diameter is 275 mm and wall thickness of 10 mm. The scale thickness was about 90 mm. The purpose of testing this object was to know the ability of the system to investigate the metal material and to recognize the scale in it. Object #2 consisted of three materials that had close density values. The densities of water, paraffin, and pertalite are 1 g/cm^3, 0.9 g/cm^3, and 0.72-0.77 g/cm^3, respectively. It was to test the ability of the system to distinguish materials with close density values.

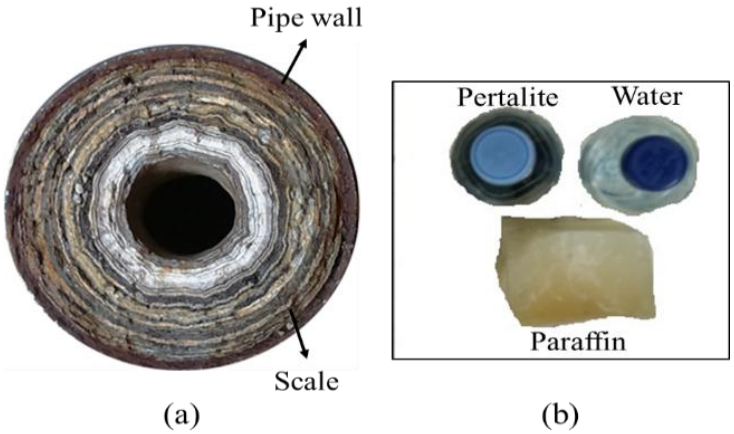

Figure 2. Experimental objects, (a) Object #1: geothermal power plant pipe with scale in it, (b) Object #2: water, paraffin, and pertalite

p ISSN 1907-0322
e ISSN 2527-6433

Both of objects were scanned to get the projections profiles. Object #1 was scanned in translational mode at 0^0. The step is every 5 mm. Each translational scan conducted 64 steps to cover all the dimension of the object. The gantry was then rotated 5.625^0 and proceed translation scan to get the next projection data. It was continued until all the 32 projections data were obtained.

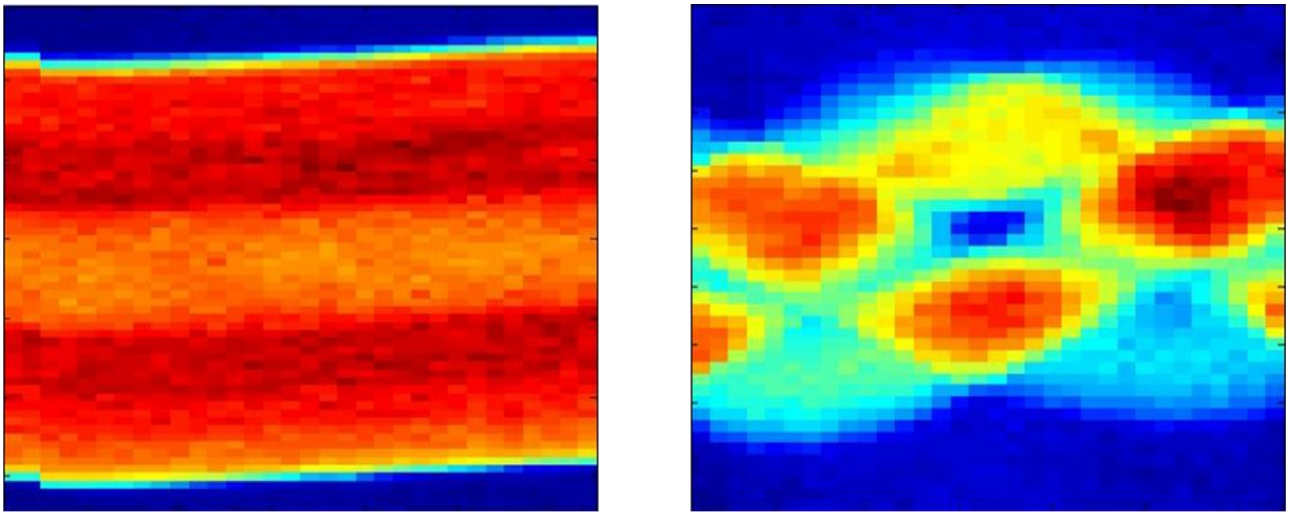

Figure 3. Sinograms, (a) object #1, (b) object #2

Image reconstruction

The 32 projections data of each object built into image using filtered back projection algorithm. The filtered back projection algorithm is a wellknown classical technique, if the fast Fourier algorithm is use then the data should be obtained in 2^n parallel rays and use of the radon transformation [14]. The Radon transform is defined as [15]

$$R(f) = \int_{-\infty}^{\infty}\int_{-\infty}^{\infty} f(x,y)\delta(x\cos\theta + y\sin\theta - t)dxdy \quad (2)$$

the line integral along a line (gamma-ray beam) at an angle θ from the x-axis and at a distance t from the origin as shown in Figure 4, then:

$$t = x\cos\theta + y\sin\theta \quad (3)$$

$$s = -x\sin\theta + y\cos\theta \quad (4)$$

$$x = t\cos\theta - s\sin\theta \quad (5)$$

$$y = t\sin\theta + s\cos\theta \quad (6)$$

image obtained by restoring the value of radon to the x,y-axis by using the inverse radon (iradon)

$$\mu(x,y) = \int_{0}^{\pi} P\theta(t)\int_{-\infty}^{\infty}\delta(x\cos\theta + y\sin\theta - t)dtd\theta \quad (7)$$

Image building process as shown in Figure 5. The radon transformed from the object was then converted into the inverse radon. With a number of object's inverse Radon data, the object can be imaged.

p ISSN 1907-0322
e ISSN 2527-6433

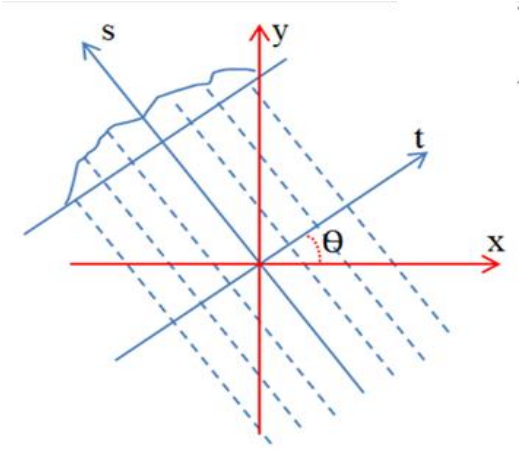

Figure 4. Image coordinate system.

Filtered back projection algorithm contain two steps: convolving each projection with a 1-dimensional (1D) filter and then backprojecting the filtered projections to obtain a clear image [16] as shown in Figure 6. The filter was designed to operated directly in the frequency domain and then multiplied by the Fast Fourier Transform (FFT) of the projections. The projections are zero-padded to a power of 2 before filtering to prevent spatial domain aliasing and to speed up the FFT.

The basic filter used in this paper was Ramp filter. The Ramp filter is defined as [17]

$$q(\omega) = \frac{\omega}{2\pi} \tag{8}$$

where ω is the spectral window. The other filters used were Shepp-logan, Hann, Hamming, and Cosine filter. The Shepp-Logan filter multiplies the Ramp filter by a sine function, Hann filter multiplies Ramp filter by Hann window, Hamming filter multiplies Ramp filter by Hamming window, and the Cosine filter multiplies the Ramp filter by a cosine function.

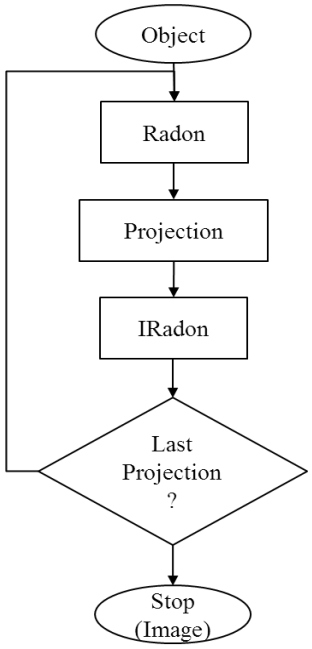

Figure 5. Back projection image reconstruction process

p ISSN 1907-0322
e ISSN 2527-6433

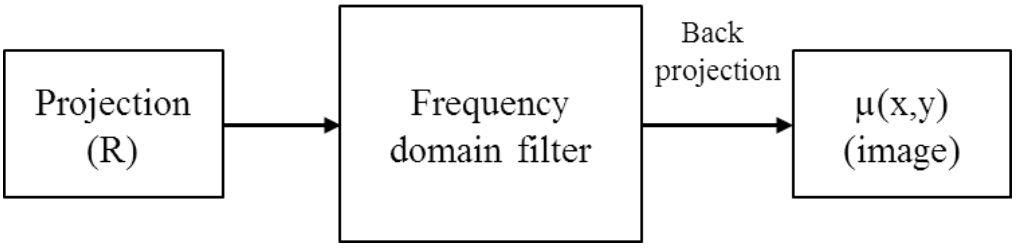

Figure 6. Projection frequency domain filtering process

RESULTS AND DISCUSSION

Image reconstruction results of both objects showed effect of filters to image quality. Object #1 is steel pipe with scale in it. The aims of object #1 measurements were to test the ability of gamma tomography system to investigate material with high density (pipe and scale) and to observate the effect of filters at the images reconstruction. Object #1 projections data built into image six times. First was using back projection algorithm (with no filter), then using filtered back projection algorithm with Ramp filter, Shepp-logan filter, Hann filter, Hamming filter, and Cosine filter, respectively.

Based the visual observation of the reconstructed image of object #1, image result with no filter looked blur. The difference of density between pipe wall and scale was difficult to recognize as shown in Figure 7 (a). Void area (air) at the centre of the pipe was not very clear. The image was too bright looked like luminous. Compared with the object, the image reconstruction with no filter did not represent the cross-sectional spatial patterns. The solid objects represented by bright white color and air represented by dark color.

The second reconstructed image using Ramp filter as shown in Figure 7 (b). The result looked much better than the image with no filter. The density difference between pipe wall, scale, and air can be clearly observed. The next four images were using Shepp-logan, Hann, Hamming and Cosine filters respectively as shown in Figure 7 (c) to (f). Based on visual observation the results were much better than image with no filter. The cross-sectional spatial patterns can be recognized like pipe wall, scale and air. The images look smoother than using Ramp filter.

Pixel value of object #1 was analyzed. Pipe wall and void (air) pixel were counted at no filter condition and using all filters have mentioned above. The data is shown in Table 1. The average pixel value of pipe wall is about 240 and void is about 39. The pixel value of void of no filtered image is quietly different from others. It is about 195 while other is about 39. It means the resolution of no filter image is very low regarding the gap of pipe wall and void pixel values.

Figure 9 shows the gaps of pixel values of pipe wall and void from object #1 images. The smallest gap is image with no filter that makes the image is not good. Then what will be discussed are the filtered images. The lowest pixel value of void was generated by Hann filter (31.56), while the highest was from Ramp filter (51.11). The highest pixel value of pipe wall was generated by Hann filter and the lowest was by Ramp filter. It means Hann filter has the highest resolution regarding to recognize the density of the object while Ramp filter has the lowest resolution among of all filtered images.

Standard deviation of filtered images of object #1 are shown in Table 1. Hann filter has the lowest standard deviation while Ramp filter has the highest standard deviation. Standard deviation of Hann filter pixel values are 3.86 for void area and 7.23 for pipe wall. Overall, Hann filter was produced the lowest standard deviation. Sequence of filters that produces images with the lowest to highest standard deviation are Hann, Hamming, cosine, Shepp-Logan, and Ramp filters.

p ISSN 1907-0322
e ISSN 2527-6433

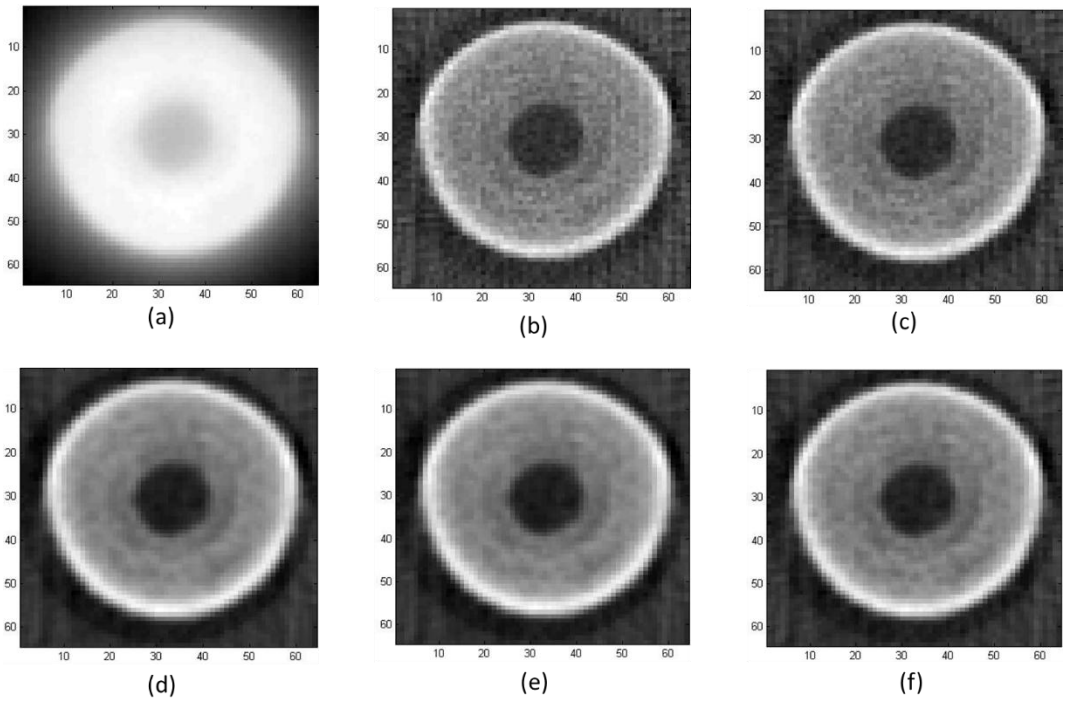

Figure 7. Image reconstruction of object #1, (a) no filter, (b) Ramp filter, (c), Shepp-logan filter, (d) Hann filter, (e) Hamming filter, (f) Cosine filter

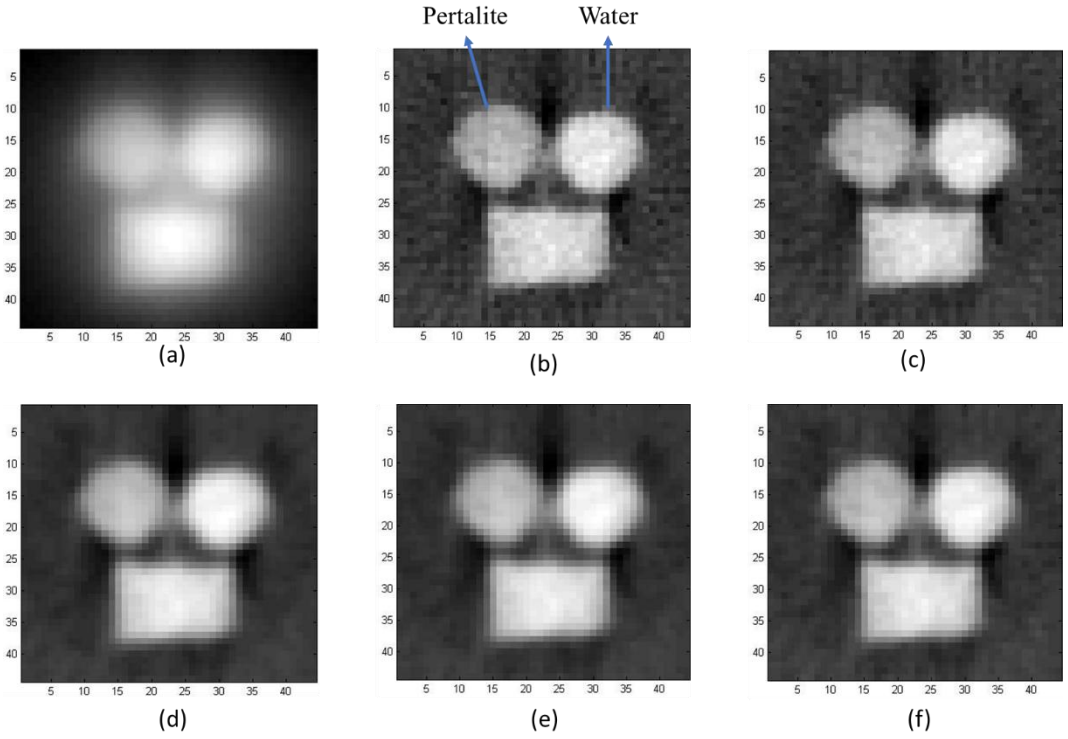

Figure 8. Image reconstruction of object #2, (a) no filter, (b) Ramp filter, (c), Shepp-logan filter, (d) Hann filter, (e) Hamming filter, (f) Cosine filter

p ISSN 1907-0322
e ISSN 2527-6433

Table 1. Image analysis of object #1

Filter	Pixel value	
	Pipe wall	Void (air)
None	237.18 ± 4.00	194.69 ± 4.48
Ramp	232.09 ± 14.29	51.11 ± 5.51
Shepp-Logan	238.36 ± 12.85	43.76 ± 4.73
Hann	248.64 ± 7.23	31.56 ± 3.86
Hamming	246.09 ± 8.63	32.04 ± 3.34
Cosine	242.36 ± 12.82	36.11 ± 3.44

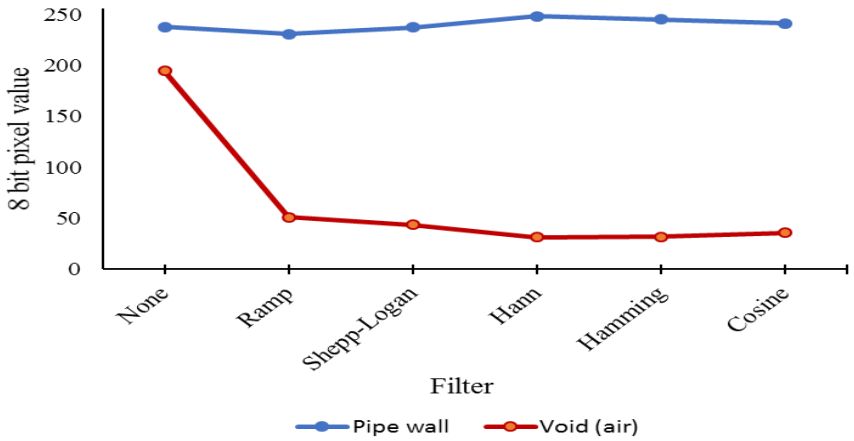

Figure 9. Pixel value of pipe wall and void area on object #1

Table 2. Image analysis of object #2.

Filter	Pixel value		
	Paraffin	Pertalite	Water
None	249.23 ± 5.54	196.75 ± 7.97	236.52 ± 8.67
Ramp	223.74 ± 8.99	184.66 ± 9.23	232.06 ± 9.33
Shepp-Logan	227.27 ± 7.40	186.28 ± 8.34	234.98 ± 8.25
Hann	237.17 ± 4.41	192.55 ± 6.94	245.40 ± 5.45
Hamming	236.65 ± 4.67	191.48 ± 7.63	244.57 ± 5.66
Cosine	233.60 ± 4.63	190.40 ± 7.51	241.75 ± 6.72

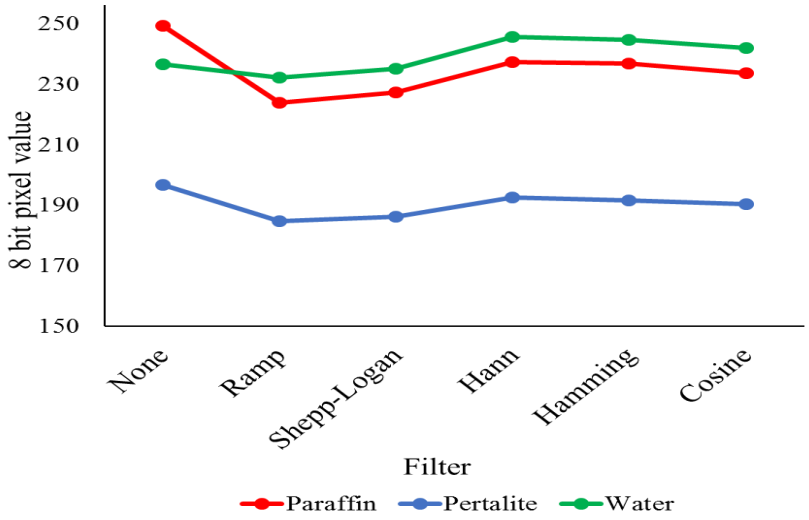

Figure 10. Pixel value of paraffin, pertalite, and water on object #2

p ISSN 1907-0322
e ISSN 2527-6433

The aims of object #2 measurements were to test the ability of gamma tomography system to investigate three materials with adjacent density values. The materials were water (1 g/cm^3), paraffin (0.9 g/cm^3), and pertalite (0.72-0.77 g/cm^3). Based on the results, the gamma tomography system using Cs-137 was successfully identified the adjacent density values. The Cs-137 gamma source with the activity of 662 keV is effective for use in industrial gamma tomography system. It can penetrate material with high density and can distinguish the material with the strength different density value.

The result with no filter was the same with object #1. The image looked blurly as shown in Figure 8 (a). It was difficult to recognize the density difference of the object although pertalite color was a little bit different (darker than others). It was looked like a shadow of light around objects.

When filtered back projection algorithms were used, the density difference of the objects can be recognized as shown in Figure 8 (b)-(f). The Ramp filter's result showed there were three objects with different values in gray scale as shown in Figure 8 (b). Water has the highest density in the object was represented by bright white color. Pertalite was represented by darker color because it has the lowest density although paraffin was between them. The image looked like it was filled with freckles. The result using Shepp-Logan filter looked smoother than using Ramp filter (Figure 8 (c)). Image from Hann, Hamming, and Cosine (Figure 8 (d)-(f)) are better than others.

Pixel value of object #2 images as shown in Table 2. The largest gap between water and paraffin pixel values was from Ramp filtered image followed by Hann, cosine, Hamming, and Shepp-logan filter was produced the smallest gap. The largest gap between pertalite and paraffin was from hamming filtered image followed by Hann, Cosine, Shepp-logan, and Ramp filtered image. For gaps between pertalite and water were Hamming, Hann, Cosine, Shepp-logan, and Ramp filtered images respectively from the largest to the smalest.

The standard deviation if pixel values of object #2 images are presented in Table 2. The overal smallest standard deviation of pixel values of object #2 was produced from Hann filtered image followed by Hamming, Cosine, Shepp-logan, and Ramp filtered images.

CONCLUSION

Image reconstruction using back projection algorithm successfully showed cross-sectional profile of the object but can not show the difference of density distribution of the object. The algorithm produced blur at image and there was a shadow of light around the object. Filtered back projection algorithm resolved the problem by using a convolution filter. The image can show the density difference of the objects. Filters are very important in image reconstruction process. It enhances the quality of the resulting image. Ramp filter's image looks like it was filled with freckles. Shepp-Logan filter produces smother image than Ramp filter. Furthermore, Hann, Hamming, and Cosine filtered images were smoother than the others.

According to object #1 and object #2 images analysis, Hann and Hamming filters produced higher resolution image regarding to recognizing density value. Hann filtered images also has the smallest standard deviation. Overall, Hann filter is recommended to reconstruct images from projections.

ACKNOWLEDGEMENTS

The authors would like to acknowledge that the Center for Isotopes and Radiation Aplication, BATAN has provided fund and other support for this study.

REFERENCES

[1] B. Azmi, Wibisono, and A. H. Saputro, "Portable Gamma Ray Tomography System for Investigation of Geothermal Power Plant Pipe Scaling," *2017 15th Int. Conf. Qual. Res. Int. Symp. Electr. Comput. Eng.*, pp. 159-163, 2017.

[2] D. N. The Duy, N. H. Quang, P. Van Dao, B. T. Duy, and N. Van Chuan, "A Third Generation Gamma-ray Industrial Computed Tomography Systems for Pipeline Inspection," *J. Teknol.*, vol. 17, pp. 49-53, 2015.

[3] S. V. Chakhlov, S. P. Osipov, A. K. Temnik,

p ISSN 1907-0322
e ISSN 2527-6433

and V. A. Udod, "The current state and prospects of X-ray computational tomography," *Russ. J. Nondestruct. Test.*, vol. 52, no. 4, pp. 235-244, 2016.

[4] G. A. Johansen, *Radioisotope Gauges for Industrial Process Measurements*. John Wiley & Sons, Ltd, 2004.

[5] M. Khorsandi and S. A. H. Feghhi, "Design and construction of a prototype gamma-ray densitometer for petroleum products monitoring applications," *Meas. J. Int. Meas. Confed.*, vol. 44, no. 9, pp. 1512–1515, 2011.

[6] [6] H. Shahabinejad, S. A. H. Feghhi, and M. Khorsandi, "Structural inspection and troubleshooting analysis of a lab-scale distillation column using gamma scanning technique in comparison with Monte Carlo simulations," *Measurement*, vol. 55, pp. 375-381, 2014.

[7] [7] T. Al-Juwaya, N. Ali, and M. Al-Dahhan, "Investigation of cross-sectional gas-solid distributions in spouted beds using advanced non-invasive gamma-ray computed tomography (CT)," *Exp. Therm. Fluid Sci.*, vol. 86, pp. 37-53, 2017.

[8] M. K. Al Mesfer, A. J. Sultan, and M. H. Al-Dahhan, "Impacts of dense heat exchanging internals on gas holdup cross-sectional distributions and profiles of bubble column using gamma ray Computed Tomography (CT) for FT synthesis," *Chem. Eng. J.*, vol. 300, pp. 317-333, 2016.

[9] Q. Xue, H. Wang, C. Yang, and Z. Cui, "Experimental research on two-phase flow visualization using a low-energy gamma CT system with sparse projections," *Meas. Sci. Technol.*, vol. 24, no. 7, 2013.

[10] G F. Knoll, *Radiation Detection and Measurement*, 2nd ed. John Wiley & Sons, Ltd, 2010.

[11] I. M. Orlov, D. G. Morgan, and R. H. Cheng, "Efficient implementation of a filtered back-projection algorithm using a voxel-by-voxel approach," *J. Struct. Biol.*, vol. 154, no. 3, pp. 287-296, 2006.

[12] J. Kim, S. Jung, J. Moon, and G. Cho, "Industrial gamma-ray tomographic scan method for large scale industrial plants," *Nucl. Instruments Methods Phys. Res. Sect. A Accel. Spectrometers, Detect. Assoc. Equip.*, vol. 640, no. 1, pp. 139-150, 2011.

[13] B. Azmi, Wibisono, and A. H. Saputro, "Measurement of Pipe Scaling using Parallel Beam Gamma Tomography," *A Sci. J. Appl. Isot. Radiat.*, vol. 13, pp. 1–10, 2017.

[14] J. Abdullah, M. C. F. Cassanello, M. P. Dudukovic, T. Dyakowski, M. M. Hamada, J. H. Jin, G. a. Johansen, J. B. Kim, S. a. Legoupil, R. Maad, C. . Mesquita, J. Nowakowski, F. P. Ramirez-Garcia, D. Sankowski, S. M. Sipaun, and J. Thyn, "Industrial Process Gamma Tomography," *IAEA-Tecdoc-1589*, 2008.

[15] D. N. The Duy, N. H. Quang, P. Van Daon, B. T. Duy, and N. Van Chuan, "A Third Generation Gamma-ray Industrial Computed Tomography Systems for Pipeline Inspection," *J. Teknol.*, vol. 17, pp. 49-53, 2015.

[16] Z. Wang and I. Lee, "Backprojection regularization with weighted Ramp filter for tomographic reconstruction," *Proc. Annu. Int. Conf. IEEE Eng. Med. Biol. Soc. EMBS*, vol. 2015–November, no. 4, pp. 7039-7042, 2015.

[17] S. Horbelt, M. Liebling, and M. Unser, "Filter design for filtered back-projection guided by the interpolation model," *Proc. SPIE*, no. August 2015, pp. 806-813, 2002.

p ISSN 1907-0322
e ISSN 2527-6433